Journal of Materials Chemistry B

ROYAL SOCIETY OF CHEMISTRY

PAPER

View Article Online
View Journal | View Issue

Cite this: J. Mater. Chem. B, 2024, 12, 9930

Simultaneous detection of breast cancer biomarkers HER2 and miRNA-21 based on duplex-specific nuclease signal amplification†

Miao He,‡[a] Zhiqiang Hou,‡[a] Feifan Yin,[a] Wenting Cheng,[a] Yang Xiang *[ab] and Zhongyun Wang*[c]

Received 15th August 2024,
Accepted 3rd September 2024

DOI: 10.1039/d4tb01845a

rsc.li/materials-b

The detection of a single biomarker is prone to false negative or false positive results. Simultaneous analysis of two biomarkers can greatly improve the accuracy of diagnosis. In this work, we designed a new method for coinstantaneous detection of two breast cancer biomarkers miRNA-21 and HER2 using the properties of duplex-specific nuclease (DSN). Cy5-labeled DNA1 and FAM-labeled DNA2 are used as signal probes to distinguish the two signals. When the sample contains the targets HER2 and miRNA-21, HER2 binds to the HER2 aptamer on the double-stranded DNA2, while miRNA-21 binds to the complementary DNA1. Then, DSN enzyme is added to cut the DNA probes adsorbed on the HER2 aptamer and miRNA-21, releasing the fluorescent groups, which can be readsorbed to the empty sites, thus repeating the cutting of the probes and producing an exponential signal amplification with two distinct fluorescent signals. The detection limits of miRNA-21 and HER2 are 1.12 pM and 0.36 ng mL^{-1}, respectively, with linear ranges of 5 pM to 50 pM and 1 ng mL^{-1} to 15 ng mL^{-1}. The method was validated in real biological samples, providing a new approach for synchronous analysis of important markers in breast cancer.

1. Introduction

Breast cancer is one of the most common malignancies and the second leading cause of cancer death in women.[1] The human epidermal growth factor receptor family consists of four structurally related members:[2] HER1 (ErbB1, also known as (EGFR)), HER2 (ErbB2), HER3 (ErbB3), and HER4 (ErbB4).[3] In particular, HER2 has been confirmed as one of the most common malignant tumor markers in various tumors.[4,5] It is overexpressed in the tissues of breast cancer patients and it can stimulate the abnormal growth of breast cancer cells.[5] The analysis and detection of HER2 expression in tumor tissues has been used as an independent indicator of clinical diagnosis and treatment of tumors. So, it has high diagnostic value, and has received more and more attention at present.[6] At present, sensing research on HER2 is gradually developing.[7] However, the individual HER2 detection was not comprehensive enough to cause false positive results.

miRNA-21 expression is associated with multiple cancers. For example, miRNA-21, in hepatocellular carcinoma-derived exosomes, promotes tumor progression by transforming hepatocellular stellate cells into cancer-associated fibroblasts.[8] miRNA-21 has also been used as a marker for lung cancer.[9] The miRNA-21 expression has been reported to be significantly higher in human breast cancer than in healthy individuals,[10] and its expression is associated with tumor progression and poor prognosis.[11–13] In recent years, miRNA-21 research has been used as a biomarker for early disease diagnosis,[14–16] resulting in the development of a variety of biosensors for miRNA-21 detection.[14,17–19]

In addition to the traditional methods, a lot of detecting techniques,[20–22] about miRNA or protein, are constantly being studied. For example, miRNA was analyzed using laser-induced graphene electrochemical microfluidic chips and series multiplexing techniques, which provided new ideas for the expansion and development of high-performance miRNA biosensors.[23,24] However, miRNAs have low abundance, small size, sequence homology among miRNA family members, and are highly degradable, which makes their analysis still challenging.[19,25,26] A special biomolecular immobilized carrier, such as magnetic beads (MBs), which can be easily separated with magnets in a short period of time, can be used so

[a] State Key Laboratory of Pharmaceutical Biotechnology, School of Life Sciences, Nanjing University, Nanjing 210023, P. R. China. E-mail: xiangy@nju.edu.cn
[b] State Key Laboratory of Natural and Biomimetic Drugs, Peking University, Beijing 100191, P. R. China
[c] Department of Anesthesiology, The First Affiliated Hospital of Nanjing Medical University, Nanjing 210029, P. R. China. E-mail: zywang1970@126.com

† Electronic supplementary information (ESI) available. See DOI: https://doi.org/10.1039/d4tb01845a

‡ These authors contributed equally to this work.

that the background signal is reduced.[27–29] In addition, double strand specific nuclease (DSN enzyme) assisted target cyclic amplification has been used as an isothermal signal amplification method for miRNA detection.[30–32] DSN showed strong specific cleavage activity for DNA in double-stranded nucleic acid.[30,33] For example, it does not cut RNA, but effectively cuts strands of DNA in ref. 34 and 35. DSN enzymes, meanwhile, are able to distinguish between non-perfectly paired double-stranded and perfectly paired double-stranded DNA, which makes DSN enzyme-based biosensing analysis ultra-selective.[35–37] To sum up, the detection of two disease markers, using magnetic beads and DSN enzymes, is an urgent need for breast cancer.

In this part of the work, we used double-stranded specific nucleases and magnetic beads to build a highly selective, multi-fluorophore, multi-target simultaneous detection biosensor for the detection of two different targets, namely miRNA-21 and HER2. To be specific, we designed two kinds of DNA signal probes, in which DNA1 was labeled by Cy5 and DNA2 was labeled by FAM. The 3′ segment of both signal probes was modified by biotin, and biotin could covalently bind with avidin on magnetic beads to form functional magnetic beads. When HER2 and miRNA-21 are present, they are analyzed separately and simultaneously, producing two highly different fluorescence signals. Double-stranded specific nucleic acids selectively hydrolyze the hybridized DNA regions in double-stranded DNA and DNA-RNA, which can realize the recycling of miRNA, so that the signal output is efficient and fast. This method can be used for single detection of HER2 or miRNA-21, and there is no cross-reaction between the two signal probes during detection. This method also shows good selectivity for base mismatch, and has high stability and specificity for the detection of HER2 and miRNA-21 in serum samples. This double-target detection method is expected to provide a reference for breast cancer research.

2. Experimental

2.1. Materials and reagents

All oligonucleotides were fabricated and purified by Sangon Biotech Co., Ltd (Shanghai, China). Detailed sequences are listed in Table S1 (ESI†). Streptavidin-modified magnetic beads (2.8 μm, 10 mg mL^{-1}), penicillin, and streptomycin were supplied by Beaver biomedical engineering Co., Ltd (Suzhou, China). DSN enzyme, 10× DSN Reaction Buffer, and 2× DSN Stop Buffer were purchased from Costan Biotechnology Co., Ltd (Wuhan, China). Ethylene diamine tetra acetic acid (EDTA) was supplied by Beaver biomedical engineering Co., Ltd (Suzhou, China). The HER2 protein was bought in the Absin (Shanghai, China) bico. The HSA protein was purchased from Huamei Biological Engineering Co., LTD (Wuhan, China). The insulin was purchased from Mairel Biochemical Technology Co., Ltd (Shanghai, China). The serum samples were provided by the First Affiliated Hospital of Nanjing Medical University and approved by the Ethics Committee. The phosphate-buffered saline (PBS) buffer was purchased from Aladdin Biochemical Technology Co., Ltd (Shanghai, China). Tris-HCl buffer (PH 7.5) was obtained from Sangon Biotech Co., Ltd (Shanghai, China). 6× GelstainRed Prestain was obtained from UE Biotechnology Co., Ltd (Suzhou, China).

2.2. Instrumentation

All solutions were obtained using ultrapure water (>18.25 mΩ cm^{-1}) that was prepared by a Millipore Milli-Q water purification system. The GenoSens1880 gel imaging analysis system for imaging was from Qinxiang Scientific Instrument Co., Ltd (Shanghai). The B-20r bench centrifuge was from NACHT company (Germany). Thermostatic mixing apparatus was from YouNing instrument Co., Ltd (Hangzhou). FA1204B electronic balance instrument was from Co., Ltd (Shanghai). An FE20 laboratory pH meter (Shanghai mettler Toledo instrument Apparatus Co., Ltd) was used. Electrophoresis tank: a VE-180 miniature vertical electrophoresis tank from Tanon life science Co., Ltd (Shanghai). All fluorescence emission spectra were measured with the infinite M200 PRO Multimode Reader (TECAN, Switzerland).

2.3. Assembly of functional magnetic beads for dual signal probe coupling

Probe DNA-modified Fe_3O_4 magnetic beads (probe-MBs) were prepared. First, a bottle containing 2.8 μm streptavidin magnetic beads was placed on a vortex oscillator for 20 seconds and oscillated to re-suspend the beads. Then, a pipette was used to remove 100 μL magnetic beads into a new centrifuge tube. The centrifuge tube was placed on a magnetic separation rack and allowed to stand for more than 1 minute (this operation is referred to as magnetic separation later), and then a pipette was used to absorb the supernatant and the centrifuge tube was removed from the magnetic separator. 1 mL PBS buffer was added into the centrifuge tube, and then the centrifuge tube was covered and fully oscillated to resuspend the magnetic beads. Magnetic separation was performed, and the supernatant was removed. The above steps were repeated once. Then 1 μM DNA1 and 250 μL DNA2 solutions diluted with PBS buffer were added before fully oscillating the resuspended magnetic beads. The centrifuge tube was placed on a constant temperature mixer and rotated at room temperature for 30 minutes. Magnetic separation was then performed and the supernatant was transferred to a new centrifuge tube. The magnetic beads were washed three times with PBS buffer. According to the requirements of the follow-up experiment, 200 μL PBS solution was added to re-suspend the magnetic beads.

2.4. Gel electrophoresis

The 12% polyacrylamide electrophoresis gel was made using 1× TrisBorate-EDTA (TBE) buffer. An 8 μL sample was diluted by 1.5 μL 6× GelstainRed Prestain, and then used for gel electrophoresis. Then the gel was run at 100 V for 60 min. Then, imaging was performed by a ChemiDoc touch imaging system.

2.5 Detection of HER2 and miRNA-21

25 μL of the above magnetic bead solution was taken, 25 μL HER2 aptamer solution was added (1.5 μM), and the solution was mixed on a rotary mixer at room temperature for 45 min, so that the HER2 aptamer and DNA2 can be fully combined, and then it was washed with DEPC water three times to remove the uncombined HER2 aptamer. Then 50 μL DEPC water gravity suspended magnetic beads was added. Then, 5 μL magnetic bead solution was added to the centrifuge tube, along with 5 μL 10× DSN Reaction Buffer, 0.3 U DSN enzyme, 2.5 μL HER2 and miRNA-21 solutions with different concentrations, and then the reaction solution was supplemented to 50 μL. The centrifuge tube was placed on a constant temperature mixer and reacted at 55 °C for 120 min. After the reaction, the centrifuge tube was placed on the magnetic separation rack, and the supernatant was transferred to a 96-well plate after magnetic separation. The fluorescence value of FAM was measured by an infinite 200 pro. The excitation wavelength of FAM was 485 nm and the emission wavelength was 525 nm, while the excitation wavelength of Cy5 was 625 nm and the emission wavelength was 675 nm.

2.6 Detection of HER2 and miRNA-21 in serum samples

A certain amount of HER2 and miRNA-21 was added to human serum samples and simultaneous detection was performed. HER2, in the serum of healthy people, had different concentrations (1, 2, 5, 10 ng mL^{-1}), and miRNA-21 also had different concentrations (1, 5, 10, 20 pM). Finally, the recoveries of HER2 and miRNA-21 in human serum samples were then measured.

3. Results and discussion

3.1. Preparation of the MNP-DNA probe and the detection principle

In this experiment, magnetic beads were used as a DNA probe carrier and DSN enzyme was used as a signal amplification

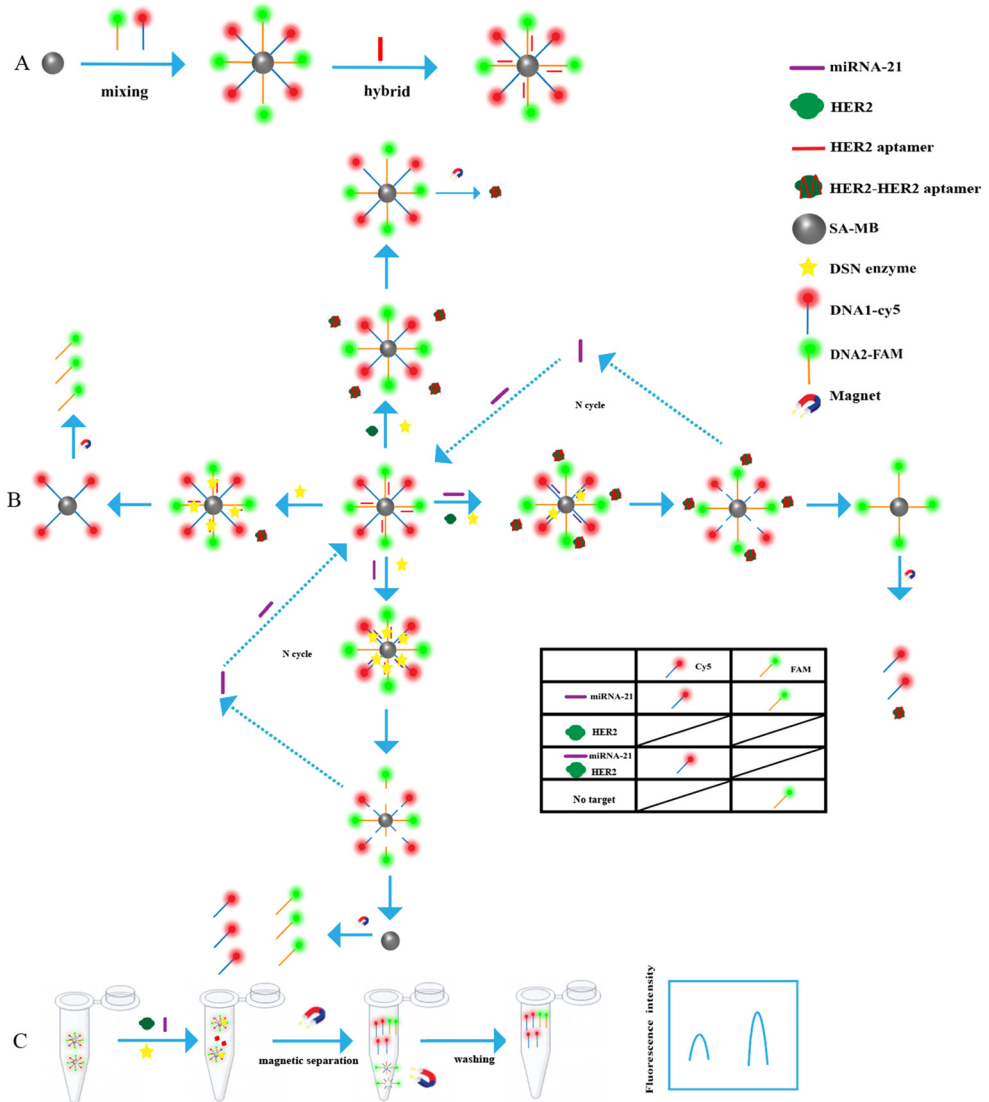

Fig. 1 Schematic diagram of simultaneous analysis of breast cancer biomarkers HER2 and miRNA-21 based on DSN. (A) Preparation of functionalized magnetic beads. (B) Test results produced by different addition methods of HER2 and miRNA-21. (C) Centrifuge tube sample test procedure.

tool (Fig. 1). Two kinds of fluorophores with high signal differentiation were selected to detect the two kinds of targets, respectively. DSN can selectively cleave DNA in double-stranded DNA and DNA–RNA hybridization strands, and DSN has the ability to distinguish between completely complementary and incomplete complementary (at most one mismatched) hybrid double-stranded DNA, and DSN has almost no activity against single-stranded nucleic acid molecules and double-stranded RNA. Two kinds of fluorescence signal probes were designed, namely DNA1-Cy5 and DNA2-FAM (Fig. 1A). The 3 'terminal of DNA1-Cy5 was labeled by Cy5, and a segment of DNA1 sequence was complementary to miRN-21, and a segment of DNA2-FAM was complementary to HER2 aptamer by FAM. Biotin was linked to the 5′ end of both signal probes, which are covalently bound to streptavidin on magnetic beads. DNA1-Cy5 and DNA2-FAM were mixed with streptavidin modified magnetic beads to form functional magnetic beads with two kinds of signal probes (Fig. 1A). When miRNA-21 and HER2 are present together, HER2 binds to the complementary HER2 Aptamer of DNA2-FAM, and miRNA-21 complements DNA1-Cy5. Adding DSN, DSN cleaved DNA probes in RNA–DNA hybridization and double-stranded DNA, releases fluorophores, and the free sites can re-adsorb the probes, thereby cyclically cutting the probes and generating exponential amplification of fluorescence signals (Fig. 1B). When only one of miRNA-21 or HER2 is present, correspondingly, the fluorescence signal of Cy5 in the supernatant was higher, or the fluorescence signal of FAM was relatively lower, after magnetic separation (Fig. 1B). The overall testing process is shown in Fig. 1C. The methods of miRNA-21 and HER2 were respectively in the two kinds of fluorescence signal as the output signal, so the signal has a high degree of differentiation, so as to improve the accuracy of detection.

3.2. Synthesis of functionalized magnetic beads and verification of DSN enzyme-specific digestion

In order to verify whether fluorescent FAM and Cy5 were successfully modified by magnetic beads in the fluorescent biosensor, Yb was measured before the fluorescence of the fluorescent-modified solution was added to the magnetic beads. Then, the fluorescence of the solution after magnetic separation was measured to obtain Ya($\Delta a = Y_b - Y_a$). The fluorescence of FAM and Cy5 decreased correspondingly (Fig. S1, ESI†). It was proved that FAM and Cy5 were modified onto magnetic beads by streptavidin and biotin. After that, we verified the hydrolyzing activity of the DSN enzyme by gel electrophoresis (Fig. 2A and B). In lane 1, miRNA-21, could not only form a single chain but also formed a stem ring structure at room temperature, which had two bands (Fig. 2A). miRNA-21 bound to DNA1-Cy5 without the addition of DSN enzyme in the third lane and would not be destroyed. After the addition of miRNA21 in the fourth lane, DSN could digest DNA in the DNA–RNA double strand and produced a tail (Fig. 2A). Similarly, the HER2 aptamer-DNA2-FAM double-stranded binding in the third lane could be digested by DSN in the fourth lane (Fig. 2B). These results confirmed that DSN enzyme could digest DNA strands in the miRNA-21-DNA1-Cy5 double-stranded and

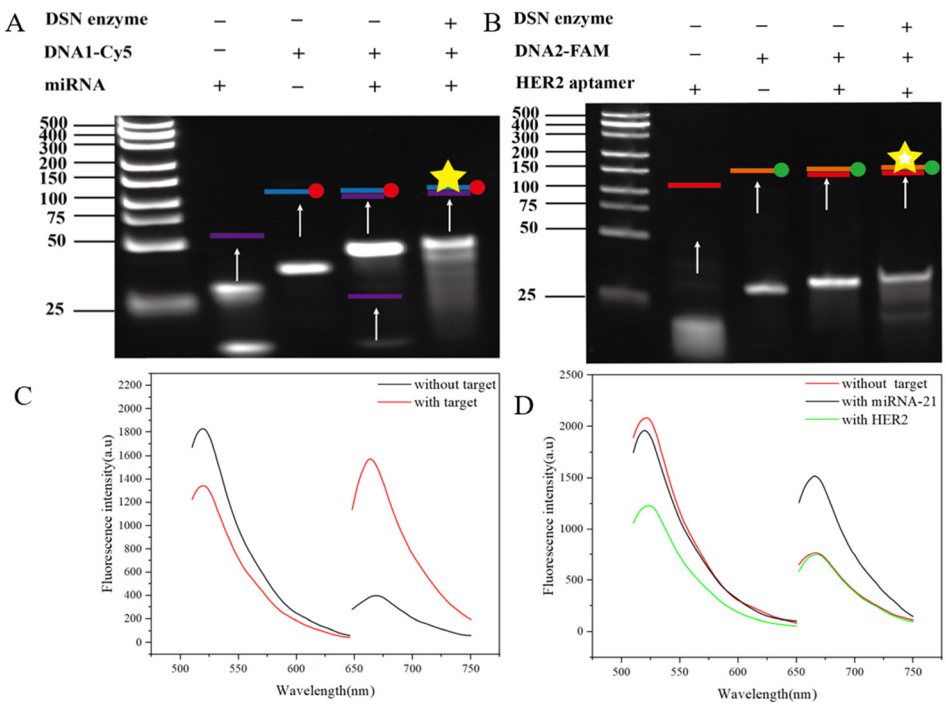

Fig. 2 Feasibility of this method for HER2 and miRNA-21 detection. (A) DNA1 could be combined with miRNA-21 and degraded by DSN. (B) DNA2 could be combined with HER2-aptamer and degraded by DSN. (C) There were 5 ng mL^{-1} HER2 and 100 pM miRNA-21, of the fluorescence spectra, when there was no target. (D) The fluorescence spectra of one target.

HER2 aptamer-DNA2-FAM double-stranded structures. The successful synthesis of functional magnetic beads was proved.

3.3. Experimental feasibility study

In order to explore the feasibility of this fluorescence biosensor in the detection of HER2 and miRNA-21, we performed a systematic fluorescence spectroscopic analysis (Fig. 2C and D). In the absence of HER2 and miRNA-21, the fluorescence signal performance of the sensor is relatively flat, and it is almost impossible to observe a significant fluorescence signal response (Fig. 2C). However, once we added HER2 (5 ng mL^{-1}) and miRNA-21 (100 pM) to the reaction system, the fluorescence signal showed a significant change (Fig. 2C). Specifically, we observed a significant reduction of the fluorescence signal at 525 nm and a significant enhancement of the fluorescence signal at 667 nm, where 525 nm and 667 nm correspond to the excitation wavelengths of the fluorescence markers FAM and Cy5, respectively. The results showed that the DSN enzyme specifically cleaved double-stranded DNA or double-stranded DNA/RNA, thus producing fluorescence signals with different effects.

In addition, to initially assess the specificity of the sensor, we further investigated whether HER2 and miRNA-21 would have cross-interference issues (Fig. 2D). When only HER2 was present, the fluorescence signal decreases significantly at 525 nm, while the signal at 667 nm remains stable. In contrast, when only miRNA-21 was present in the reaction system, the fluorescence signal was significantly enhanced at 667 nm, while the signal at 525 nm was almost unchanged. This phenomenon was a good demonstration of the sensor's anti-interference ability in detecting HER2 and miRNA-21 respectively, thus verifying its potential as a viable biosensing detection strategy.

3.4. Optimization of the experimental conditions

In order to obtain the best analysis performance and economic benefit, several key parameters were optimized, including DSN enzyme concentration, biotinylated DNA concentration when preparing functional magnetic beads, HER2 aptamer concentration, mixing time, reaction temperature, and optimization of the reaction time (Fig. 3). First, the concentration of biotinylated DNA added, during the preparation of functional magnetic beads, was optimized, and its concentration was the sum of the concentration of DNA1 and DNA2 in the same volume (Fig. 3A). The results showed that the concentration of biotinylated DNA had a direct influence on the change of fluorescence intensity of FAM and Cy5, where $\Delta F = F - F_0$, F and F_0 were fluorescence intensity in the presence and absence of target, respectively. When the concentration of biotinylated DNA added in the preparation of functional magnetic beads reached 2 μM, both 0_{FAM} and h_{Cy5} reached a plateau, indicating that the DNA loaded on the magnetic beads tended to be saturated at the concentration of 2 μM and could not continue to load more DNA. Therefore, the concentration of 2 μM of biotinylated DNA was both the most economical concentration and the optimal concentration for the reaction. Then we optimized the concentration of added HER2 aptamer (Fig. 3B). There was a limit to the amount of DNA that magnetic beads could carry. Therefore, the DNA that can complement the HER2 aptamer is limited. When the amount of added HER2 aptamer increases, er_{Cy5} maintained a relatively stable state. While la_{FAM} gradually increased, reaching the highest at 1.5 μM, the added HER2 aptamer concentration was the optimal concentration. We also optimized the mixing time after adding HER2 aptamer (Fig. 3C). With the increase of the mixing time, 3_{FAM} gradually increased, and Δ_{Cy5} always maintained a stable level. When the time reached about 45 min, F_{FAM} reached a plateau, so 45 min

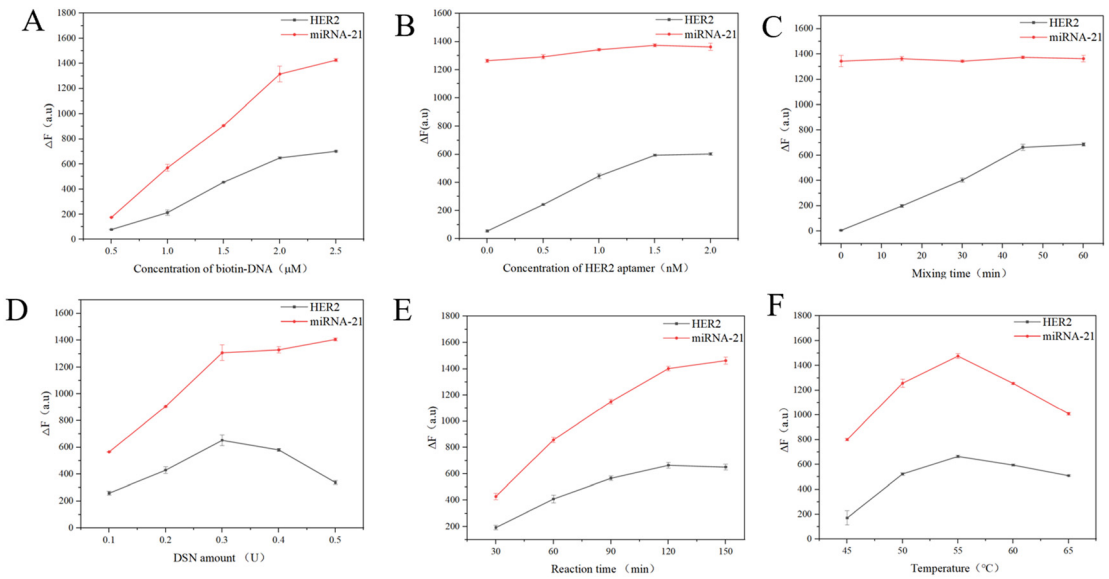

Fig. 3 Optimization of the experiment for the proposed sensor. (A) Biotin-DNA concentration. (B) HER2 aptamer concentration. (C) Mixing time after adding the HER2 aptamer. (D) DSN concentration. (E) Reaction time. (F) Reaction time. The data error bars indicate mean ± SD (n = 3).

was the best time for mixing. The above two-step optimization also indirectly indicates that there was almost no cross interference between HER2 and miRNA-21.

Subsequently, we optimized the concentration of DSN enzyme (Fig. 3D). The results showed that with the increase of DSN enzyme concentration, or_{Cy5} showed an upward trend and reached a plateau at about 0.3 U, while n_{FAM} showed a trend of first increasing and then decreasing, reaching the peak at 0.3 U, which would be related to the increase of background signal. Therefore, we took 0.3 U as the optimal concentration of DSN. Then we optimized the reaction time (Fig. 3E). With the increase of reaction time, 3_{FAM} and th_{Cy5} both showed an upward trend and reached the plateau at 120 min, indicating that the optimal reaction time was 120 min. Finally, we optimized the reaction temperature (Fig. 3F). When the temperature gradually rised, ΔF would reach its peak at 55 °C, and then gradually decreased, indicating that DSN was more sensitive to temperature. Thus, 55 °C was the most suitable reaction temperature.

In brief, the overall optimization results were as follows: when the concentration of biotinylated DNA reached 2 μM, the concentration of HER2-aptamer was 1.5 μM, the mixing time was 45 min, the concentration of DSN was 0.3 U, the reaction time was 120 min, and the reaction temperature was 55 °C, and the detection effect was the most effective.

3.5. Sensitivity analysis of HER2 and miRNA-21 separately

Under the above optimized conditions, we carried out separate quantitative determination of HER2 and miRNA-21, in order to detect the detection effect of the biosensors on HER2 and miRNA-21 respectively. The first was a separate test of HER2 (Fig. S2, ESI†). The fluorescence at 525 nm was observed with HER2 concentration from 0 nM to 5 nM. The fluorescence intensity decreased, while the fluorescence intensity at 667 nm remained constant. The linear range was from 1 ng mL^{-1} to 15 ng mL^{-1}, the detection limit (LOD) was 0.34 ng mL^{-1}, and the linear fitting equation was $F = -68.1C_{HER2} + 1825.5$, where F is the fluorescence intensity at 525 nm, R^2 = 0.9870 (Fig. S2B, ESI†).

Next, we conducted a separate detection of miRNA-21 (Fig. S3, ESI†). With the concentration of miRNA-21 from 0 nM to 5 nM, the fluorescence intensity at 667 nm increased, while the fluorescence intensity at 525 nm remained unchanged. The linear relationship, between fluorescence intensity and miRNA-21 concentration, was shown (Fig. S3B, ESI†). The linear range was from 5 pM to 50 pM, the detection limit (LOD) was 1.59 pM, and the linear fitting equation was $F = 16070.2C_{miRNA\text{-}21} + 350.1$, where F is the fluorescence intensity at 667 nm. R^2 = 0.9924.

3.6. Simultaneous sensitivity analysis of HER2 and miRNA-21

The results of simultaneous quantitative analysis of HER2 and miRNA-21 are shown (Fig. 4). When the concentration of HER2 and miRNA-21 increased, the fluorescence intensity at 525 nm gradually decreased, while that at 667 nm gradually increased. The linear fitting equations for measuring HER2 and miRNA-21 were $F_A = -65.9\ C_{HER2} + 1798.9$ (R^2 = 0.9949) and $F_B = 16836.4\ C_{miRNA\text{-}21} + 335.1$ (R^2 = 0.9894), respectively. With linear ranges from 1 ng mL^{-1} to 15 ng mL^{-1} and from 5 pM to 50 pM, the detection limits (LOD), for HER2 and miRNA-21, were 0.36 ng mL^{-1} and 1.12 pM, respectively. It could be seen that the linear range was consistent with that of HER2 and miRNA-21 alone, and the detection limits were almost consistent. This further showed that there is almost no cross interference in the simultaneous detection of HER2 and miRNA-21. At the same time, HER2 and miRNA could not only be detected separately, but also could be detected simultaneously, which would make the biosensor have more use scenarios and higher application value.

3.7. Selectivity of the detection system

Assessing selectivity is crucial for evaluating the practicality of the constructed sensing platform. We conducted selectivity experiments on the biosensor with different nucleic acids and proteins (Fig. 5). miRNA-21 with one, two, and three base mismatches, as well as miRNA-122 and miRNA-96, were used respectively, and their concentrations were all 50 pM (Fig. 5A). It could be seen that only miRNA-21 at 50 pM can achieve the

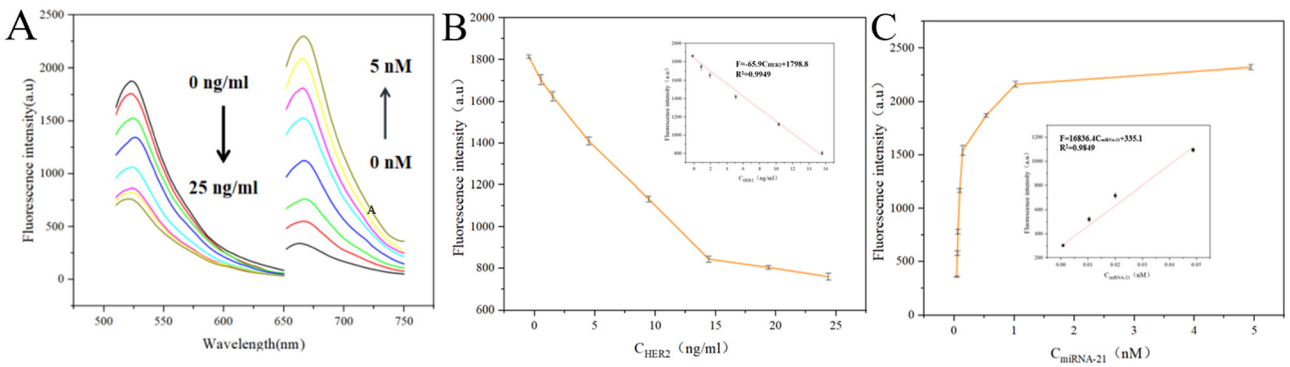

Fig. 4 Fluorescence spectra of HER2 and miRNA-21 at different concentrations were obtained at the same time. (A) Fluorescence spectra responses upon the addition of different concentrations of HER2 (0–25 ng mL^{-1}) and miRNA-21 (0–5 nM). (B) Linear relationship between fluorescence intensity and HER2 concentration. (C) Linear relationship between fluorescence intensity and miRNA-21 concentration. The data error bars indicate mean ± SD (n = 3).

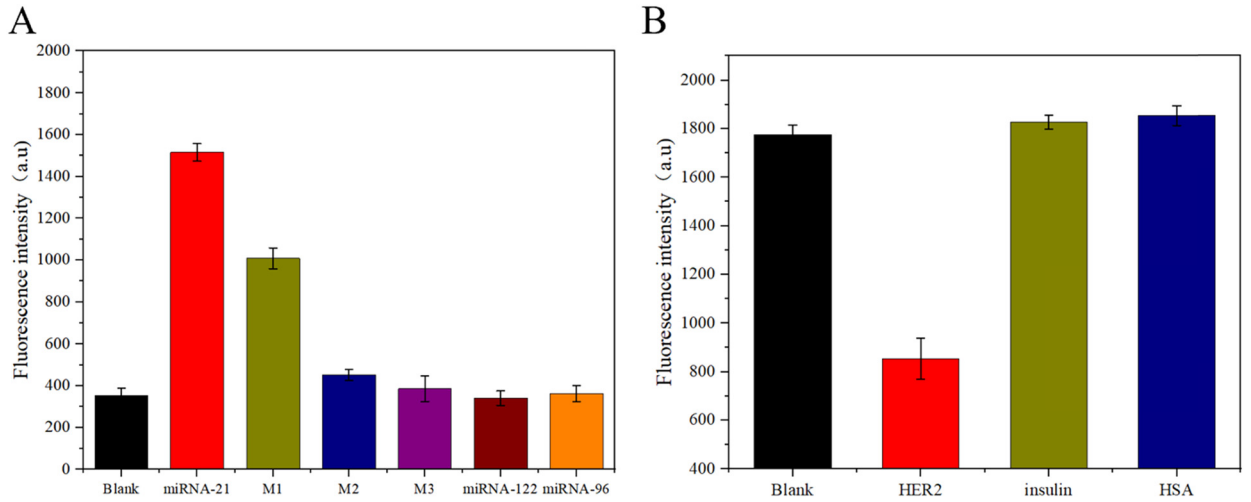

Fig. 5 Selectivity of the assay showed a significant fluorescence, compared to other miRNA and proteins. (A) Specificity of different nucleic acids. (B) Specificity of different proteins. The data error bars indicate mean ± SD (n = 3).

highest fluorescence signal. When miRNA-21 had one base mismatch, the fluorescence signal decreased significantly, while when mirNA-21 had two or three mismatches, the fluorescence signal was basically the same as that of the blank group, and the fluorescence signal was similar to that of the blank group when different miRNAs were used. The experimental results of different proteins, including insulin and human serum albumin (HSA) as controls, were detected, and the concentration of all proteins was 20 ng mL^{-1} (Fig. 5B). It could be seen that the fluorescence signal would decrease only when HER2 was present. However, the same concentration of insulin and human serum albumin hardly interfered with the fluorescence signal, which also proved the selectivity of the HER2 aptamer to HER2. In summary, the biosensor had good specificity for the detection targets.

3.8. Recovery experiment

After the verification of its theoretical detection performance, it is necessary to know the recovery rate of this detection strategy in actual serum. We added a certain amount of HER2 and miRNA-21 to human serum samples and conducted simultaneous detection (Table S2, ESI†). The experimental results showed that the recovery rates of HER2 and miRNA-21 in human serum samples ranged from 97.4% to 111.0%, which proved the reliability and potential of this method in the detection of HER2 and miRNA-21 in human serum samples.

4. Conclusions

A new method for the simultaneous detection of the dual breast cancer targets HER2 and miRNA-21 was established. This method was realized through the interaction of HER2 protein with HER2 aptamer, complementary pairing of nucleic acid bases, and DSN enzyme specific cleavage activity. Based on the ability of DSN to selectively cleave DNA in double-stranded DNA and DNA–RNA hybridization strands, and the ability of DSN to distinguish between fully complementary and not fully complementary, DSN has little activity against single stranded nucleic acid and double-stranded RNA. In this method, Cy5 labeled DNA1 and FAM labeled DNA2 were used as signal probes to distinguish two kinds of fluorescence signals. When the target HER2 and miRNA-21 were present in the sample, HER2 bound the HER2 aptamer in the HER2 aptamer-DNA2 double strand, and miRNA-21 compliantly bound DNA1. DSN was added to cleave DNA probes adsorbed on HER2 aptamer and miRNA-21, and the fluorophores were released. The free sites could readsorb the probes, so as to cut the probe cyclically, and generate exponential signal amplification with two distinct fluorescence signals. The detection limits of miRNA-21 and HER2 were as low as 1.12 pM and 0.36 ng mL^{-1}, respectively, and the linear ranges were 5 pM to 50 pM and 1 ng mL^{-1} to 15 ng mL^{-1}. The practical application capability of the method was verified in the environment of complex biological samples. It provided a novel strategy for simultaneous analysis of important markers of breast cancer.

Data availability

Data will be made available on request.

Conflicts of interest

The authors declare that they have no known competing financial interests or personal relationships that could have appeared to influence the work reported in this paper.

Acknowledgements

This work is supported by the National Natural Science Foundation of China (Grant No. 82371283, 81672570) and the State Key Laboratory of Natural and Biomimetic Drugs (Grant No. K202009).

References

1 F. Bray, J. Ferlay, I. Soerjomataram, R. L. Siegel, L. A. Torre and A. Jemal, *Ca-Cancer J. Clin.*, 2020, **70**, 313.
2 Y. Yarden and M. X. Sliwkowski, *Nat. Rev. Mol. Cell Biol.*, 2001, **2**, 127–137.
3 H. S. Cho, K. Mason, K. X. Ramyar, A. M. Stanley, S. B. Gabelli, D. W. Denney, Jr. and D. J. Leahy, *Nature*, 2003, **421**, 756–760.
4 S. S. Joshi and B. D. Badgwell, *CA Cancer J. Clin.*, 2021, **71**, 264–279.
5 S. Loibl, P. Poortmans, M. Morrow, C. Denkert and G. Curigliano, *Lancet*, 2021, **397**, 1750–1769.
6 S. E. Stanton and M. L. Disis, *J. Immunother Cancer*, 2016, **4**, 59.
7 L. Bai, C. Gu, J. Liu, P. Gai and F. Li, *Biosens. Bioelectron.*, 2023, **220**, 114850.
8 Y. Zhou, H. Ren, B. Dai, J. Li, L. Shang, J. Huang and X. Shi, *J. Exp. Clin. Cancer Res.*, 2018, **37**, 324.
9 A. Khodadoust, N. Nasirizadeh, S. M. Seyfati, R. A. Taheri, M. Ghanei and H. Bagheri, *Talanta*, 2023, **252**, 123863.
10 N. N. Kolesnikov, Y. A. Veryaskina, S. E. Titov, V. V. Rodionov, T. P. Gening, T. V. Abakumova, V. V. Kometova, M. K. Torosyan and I. F. Zhimulev, *Cancer Treat Res Commun*, 2019, **20**, 100026.
11 L. Shi, J. Li, Q. Xiang, Y. Tan, H. Zhang, S. Liu, X. Guo, W. Zhang, D. Yang and Y. Ma, *Biosens. Bioelectron.*, 2023, **237**, 115529.
12 S. Gao, H. Tian, Y. Guo, Y. Li, Z. Guo, X. Zhu and X. Chen, *Acta Biomater.*, 2015, **25**, 184–193.
13 Z. L. Zhao, Y. Cai, Y. Y. Wang, C. L. Xia, C. X. Li, S. L. Chen, Q. L. Yang and C. J. Chen, *Zhejiang Da Xue Xue Bao Yi Xue Ban*, 2015, **44**, 400–409.
14 B. Farasati Far, K. Vakili, M. Fathi, S. Yaghoobpoor, M. Bhia and M. R. Naimi-Jamal, *Life Sci.*, 2023, **316**, 121340.
15 L. Tao, X. Huang, M. Xu, Z. Qin, F. Zhang, F. Hua, X. Jiang and Y. Wang, *Mol. Cell. Endocrinol.*, 2020, **518**, 110944.
16 N. Ratnasari, P. Lestari, D. Renovaldi, J. Raditya Ningsih, N. Qoriansas, T. Wardana, S. Hakim, N. Signa Aini Gumilas, F. Indrarti, C. Triwikatmani, P. Bayupurnama, D. Setyo Heriyanto, I. Astuti and S. Mubarika Harjana, *PLoS One*, 2022, **17**, e0263298.
17 S. Yu, J. Zhang, Y. Hu, L. Li, J. Kong and X. Zhang, *Anal. Chim. Acta*, 2023, **1277**, 341661.
18 Y. Zhou, S. Xie, B. Liu, C. Wang, Y. Huang, X. Zhang and S. Zhang, *Anal. Chem.*, 2023, **95**, 3332–3339.
19 M. E. Aamri, H. Mohammadi and A. Amine, *Biosensors*, 2023, **13**(1), 74.
20 L. Liu, D. Yang and G. Liu, *Biosens. Bioelectron.*, 2019, **136**, 60–75.
21 F. Li, Y. Zhou, H. Yin and S. Ai, *Biosens. Bioelectron.*, 2020, **166**, 112476.
22 M. Liu, S. Dou, F. Vriesekoop, L. Geng, S. Zhou, J. Huang, J. Sun, X. Sun and Y. Guo, *Anal. Chim. Acta*, 2024, **1287**, 341938.
23 X. Liu, Y. Wang, Y. Du, J. Zhang, Y. Wang, Y. Xue, J. Zhao, L. Ge, L. Yang and F. Li, *Chem. Eng. J.*, 2024, **486**, 150233.
24 Y. Zhao, J. Xiang, H. Cheng, X. Liu and F. Li, *Biosens. Bioelectron.*, 2021, **194**, 113581.
25 X. Qiu, C. Liu, C. Zhu and L. Zhu, *Methods Mol. Biol.*, 2023, **2630**, 25–45.
26 H. Lu, F. Yang, B. Liu, K. Zhang, Y. Cao, W. Dai, W. Li and H. Dong, *Nanoscale Horiz.*, 2019, **4**, 472–479.
27 F. Liu, P. Kc, G. Zhang and J. Zhe, *Anal. Chem.*, 2016, **88**, 711–717.
28 A. M. Pourshahidi, S. Achtsnicht, M. M. Nambipareechee, A. Offenhäusser and H. J. Krause, *Sensors*, 2021, **21**(17), 5859.
29 Z. Fei, P. Liu, C. Cheng, R. Wei, P. Xiao and Y. Zhang, *ACS Appl. Mater. Interfaces*, 2023, **15**, 4924–4934.
30 G. Zhao, X. Yan, Y. Zhang, J. Deng and X. Liang, *Anal. Biochem.*, 2022, **654**, 114744.
31 Z. You, Z. Yang, Y. Chen and L. Zhang, *RSC Adv.*, 2021, **11**, 18068–18073.
32 Y. Zhang, P. Li, M. Hou, L. Chen, J. Wang, H. Yang and W. Feng, *Bioelectrochemistry*, 2022, **144**, 108037.
33 X. Qiu, H. Zhang, H. Yu, T. Jiang and Y. Luo, *Trends Biotechnol.*, 2015, **33**, 180–188.
34 M. Liu, H. Li, Y. Jia, P. I. Mak and R. P. Martins, *Micromachines*, 2021, 12.
35 G. Ashraf, Z. T. Zhong, M. Asif, A. Aziz, L. Song, S. Zhang, B. Liu, W. Chen and Y. D. Zhao, *Talanta*, 2022, **242**, 123314.
36 Y. Yao, H. Zhang, T. Tian, Y. Liu, R. Zhu, J. Ji and B. Liu, *Talanta*, 2021, **235**, 122728.
37 F. Xu, H. Dong, Y. Cao, H. Lu, X. Meng, W. Dai, X. Zhang, K. A. Al-Ghanim and S. Mahboob, *ACS Appl. Mater. Interfaces*, 2016, **8**, 33499–33505.